

## Strongly Coupled Phenazine-Porphyrin Dyads: Light-Harvesting Molecular Assemblies with Broad Absorption Coverage

Shin Hee Lee, Adam J. Matula, Gongfang Hu, Jennifer Troiano, Christopher Karpovich, Robert H. Crabtree, Victor S. Batista, and Gary W. Brudvig

*ACS Appl. Mater. Interfaces*, **Just Accepted Manuscript** • DOI: 10.1021/acsami.8b20996 • Publication Date (Web): 30 Jan 2019

Downloaded from <http://pubs.acs.org> on February 2, 2019

### Just Accepted

“Just Accepted” manuscripts have been peer-reviewed and accepted for publication. They are posted online prior to technical editing, formatting for publication and author proofing. The American Chemical Society provides “Just Accepted” as a service to the research community to expedite the dissemination of scientific material as soon as possible after acceptance. “Just Accepted” manuscripts appear in full in PDF format accompanied by an HTML abstract. “Just Accepted” manuscripts have been fully peer reviewed, but should not be considered the official version of record. They are citable by the Digital Object Identifier (DOI®). “Just Accepted” is an optional service offered to authors. Therefore, the “Just Accepted” Web site may not include all articles that will be published in the journal. After a manuscript is technically edited and formatted, it will be removed from the “Just Accepted” Web site and published as an ASAP article. Note that technical editing may introduce minor changes to the manuscript text and/or graphics which could affect content, and all legal disclaimers and ethical guidelines that apply to the journal pertain. ACS cannot be held responsible for errors or consequences arising from the use of information contained in these “Just Accepted” manuscripts.

1  
2  
3  
4  
5  
6  
7  
8  
9  
10  
11  
12  
13  
14  
15  
16  
17  
18  
19  
20  
21  
22  
23  
24  
25  
26  
27  
28  
29  
30  
31  
32  
33  
34  
35  
36  
37  
38  
39  
40  
41  
42  
43  
44  
45  
46  
47  
48  
49  
50  
51  
52  
53  
54  
55  
56  
57  
58  
59  
60

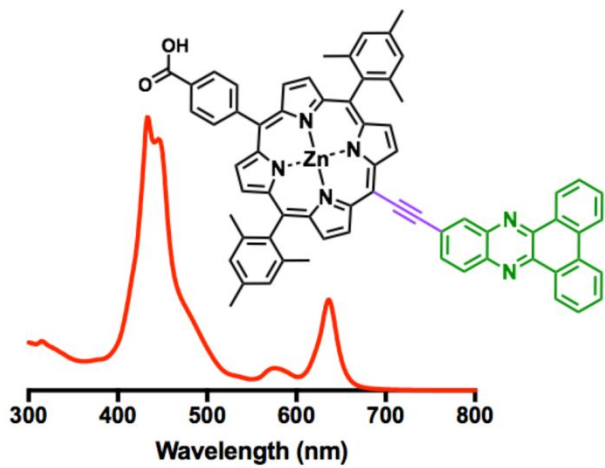
# Strongly Coupled Phenazine-Porphyrin Dyads: Light-Harvesting Molecular Assemblies with Broad Absorption Coverage

*Shin Hee Lee<sup>‡</sup>, Adam J. Matula<sup>‡</sup>, Gongfang Hu, Jennifer L. Troiano, Christopher J. Karpovich,  
Robert H. Crabtree\*, Victor S. Batista\*, and Gary W. Brudvig\**

Department of Chemistry, and Yale Energy Sciences Institute, Yale University, New Haven, CT,  
06520-8107, United States

1  
2  
3  
4  
5 KEYWORDS  
6  
78 Panchromatic dyes, dyads, phenazines, porphyrins, artificial photosynthesis.  
910  
11  
12 ABSTRACT  
13  
1415  
16 The development of light-harvesting architectures with broad absorption coverage in the visible  
17 region continues to be an important research area in the field of artificial photosynthesis. Here, we  
18 introduce a new class of ethynyl-linked panchromatic dyads comprised of dibenzophenazines  
19 coupled *ortho*- and *meta*- to tetrapyrroles with an anchoring group that can be grafted onto metal  
20 oxide surfaces. Quantum chemical calculations and photophysical measurements of the  
21 synthesized materials reveal that both of the dibenzophenazine dyads absorb broadly from 300 nm  
22 to 636 nm and exhibit absorption bands different from those of the constituent chromophore units.  
23 Moreover, the different points of attachment of dibenzophenazines to tetrapyrroles give different  
24 absorption profiles which computations suggest result from differences in the planarity of the two  
25 dyads. Applicability of the dyads in artificial photosynthesis systems was assessed by  
26 incorporation of them and characterization of their performance in dye-sensitized solar cells.  
27  
28  
29  
30  
31  
32  
33  
34  
35  
36  
37  
38  
39  
40  
41  
42  
43  
44  
45  
46  
47  
48  
49  
50  
51  
52  
53  
54  
55  
56  
57  
58  
59  
60

TOC FIGURE



## ■ Introduction

The development of artificial photosynthetic systems could benefit from a rational design of light-harvesting molecular architectures that maximally absorb solar energy and drive chemical processes for energy conversion and storage.<sup>1-5</sup> Natural photosynthetic antennas often include pigments that absorb in complementary regions of the solar spectrum to achieve an overall panchromatic absorption.<sup>6-12</sup> Previous efforts to develop artificial panchromatic systems made use of various dyads and arrays comprised of tetrapyrroles, perylenes, polycyclic and heterocyclic aromatic hydrocarbons.<sup>13-35</sup> In many cases, one or more accessory chromophores or conjugated moieties were appended to a primary non-panchromatic absorber, such as a porphyrin or a bay-annulated indigo,<sup>36</sup> via conjugated linkers, and the strong electronic coupling yielded absorption profiles considerably different from the sum of the spectra of the constituents chromophore units, affording strongly-coupled panchromatic absorbers. Design principles have been established by comparisons of newly-synthesized panchromatic dyes to well-studied dyes.<sup>23,32,37-44</sup> In this study, we made use of those principles to generate a list of possible phenazine-based tetrapyrrole dyad structures and identified the most promising candidates for extensive synthesis by computational screening and experimental characterizations.

Phenazines are highly conjugated heterocycles that can be structurally modified by many convenient synthetic methods.<sup>45-53</sup> For example, a simple condensation of *o*-phenylenediamine derivatives with functionalized *o*-quinones directly permits a variety of polyaromatic-based structures.<sup>45,46,54</sup> Accordingly, they are widely used as building blocks for a wide range of applications, including anticancer agents,<sup>55-57</sup> fluorescent markers in biological systems,<sup>58-61</sup> electroactive materials for OLEDs,<sup>50,62</sup> organic electronics,<sup>63</sup> and conductive polymers,<sup>64</sup> photoredox catalysts,<sup>65</sup> and as photoactive materials for photocatalysis and dye-sensitized solar

1  
2  
3 cells (DSSCs).<sup>66-70</sup> Phenazines are particularly attractive as light-absorbing molecules because  
4 their absorption bands can be systematically tuned by increasing the number of arene rings  
5  
6 **(Figure 1)**. However, the majority of reported phenazines have limitations from their low  
7  
8 extinction coefficients and their maximum absorption occurring in the green visible region. We  
9  
10 envisioned that one route to overcome these limitations could be the attachment of porphyrins to  
11  
12 phenazine because porphyrins exhibit high molar extinction coefficients and feature absorption  
13  
14 bands that stretch deeply into the red visible region. To ensure strong electronic perturbation  
15  
16 between the phenazine and porphyrin pigments, we chose an ethynyl linker, which is widely  
17  
18 employed in strongly coupled porphyrin architectures.<sup>41,71-78</sup> As expected from the strong  
19  
20 electronic coupling between the phenazine and the porphyrin, computations show that the  
21  
22 absorption spectrum of the dyads are different from a mere sum of the spectra of the constituent  
23  
24 fragments.  
25  
26  
27  
28  
29

30  
31 Our work fills a gap in the existing literature by demonstrating a new class of panchromatic  
32  
33 dyads comprised of phenazines coupled to tetrapyrroles with an anchoring group that can be  
34  
35 grafted onto metal oxide surfaces. In many other panchromatic dyad systems, the two constituent  
36  
37 chromophores are chosen to have complementary absorption profiles, and typically both  
38  
39 components are strongly absorbing. The phenazine used here has a low molar absorption  
40  
41 coefficient and absorbs to the blue side of the Soret band, but it is still capable of perturbing the  
42  
43 porphyrin's electronic structure enough to create all new bands in the red region of the visible light  
44  
45 spectrum. By designing and synthesizing two simple dyads of this type and evaluating their  
46  
47 potential as photosensitizers, we offer a proof-of-concept for this new class of dye, which can be  
48  
49 further tuned with structural modifications to improve performance, opening up the design space  
50  
51 for panchromatic dyes significantly. We thoroughly characterize the electronic and photophysical  
52  
53  
54  
55  
56  
57  
58  
59  
60

properties of these new panchromatic dyes, and we integrate them into dye-sensitized solar cells to characterize their performance in such systems.

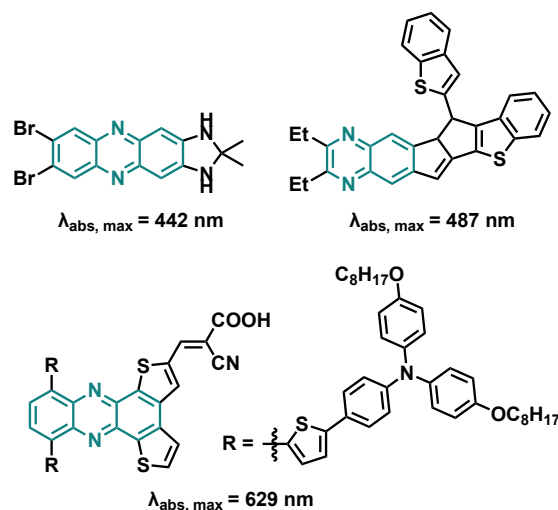


**Figure 1.** Examples of phenazines developed by Crabtree,<sup>51</sup> Hashmi,<sup>5</sup> and Zhou<sup>79</sup> (clockwise from top left) and their maximum absorption wavelengths.

## Results and Discussion

### Molecular Design and Synthesis.

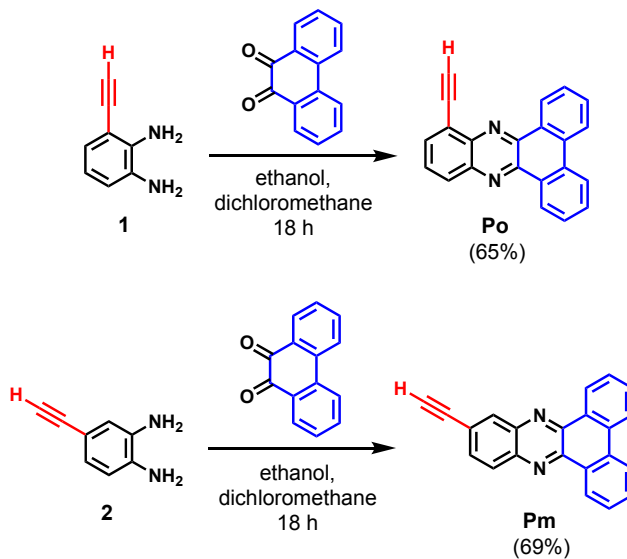
The structures of phenazine-porphyrin dyads **PoZ** and **PmZ** (**Schemes 1 and 2**) were generated using literature-supported design principles that include: (1) the creation of an extended  $\pi$ -conjugation system to broaden and red-shift the absorption bands,<sup>80,81</sup> (2) the reduction of the symmetry of a tetrapyrrole unit to accomplish the same effect as the previous principle, (3) use of the more electron-rich *meso*-site of the porphyrins for dye linkage to afford greater panchromaticity than would be achieved using the  $\beta$ -site,<sup>23,80</sup> (4) use of an ethynyl linker and coplanar constituents to maximize orbital mixing and thus electronic communication,<sup>41,71-78</sup> and (5) use of one large constituent rather than a number of smaller chromophore constituents which

1  
2  
3 has been more effective in broadening the absorption bands of a dye.<sup>80</sup> For many of the design  
4 principles, we used DFT calculated UV-Vis spectra to verify their applicability to our specific  
5 systems.  
6  
7  
8

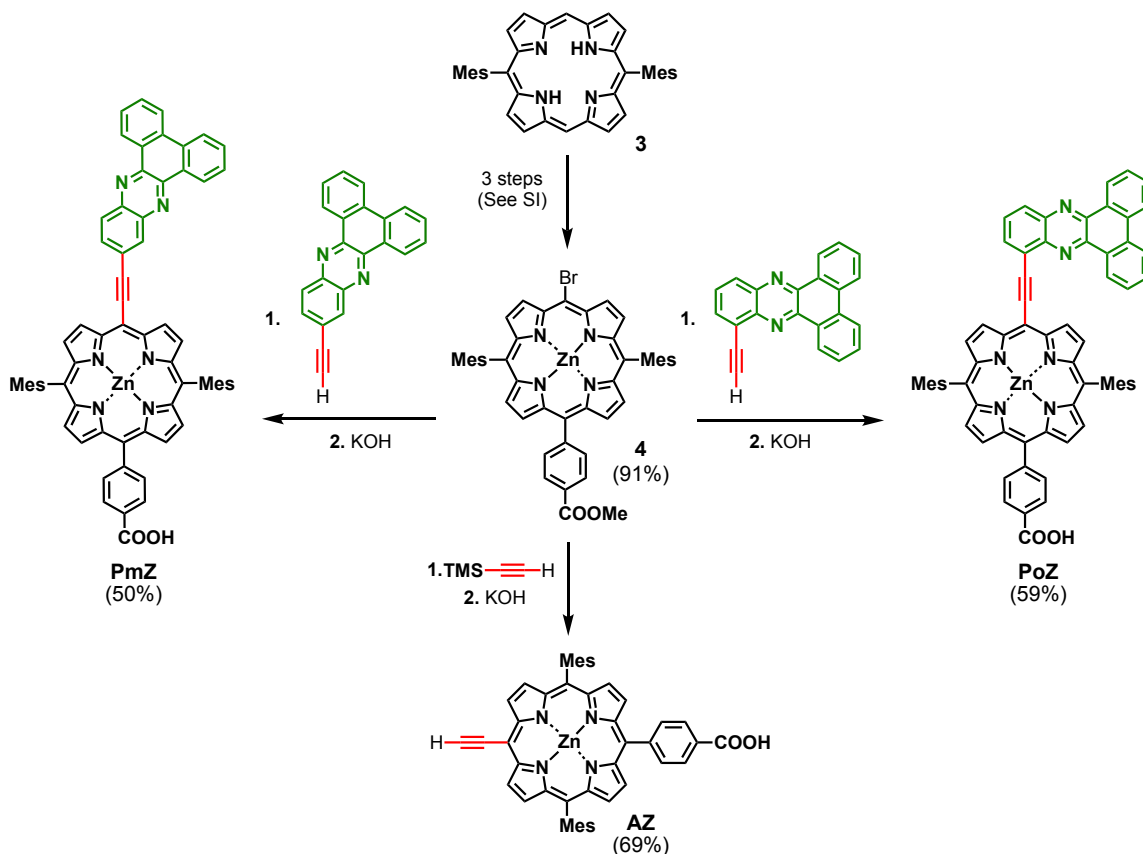
9  
10 Each of the dyads has a dibenzophenazine connected either *ortho* or *meta* to a zinc tetrapyrrole  
11 via an ethynyl linker at one *meso* position, two mesityl groups attached to *meso* positions of the  
12 tetrapyrrole *trans* to each other, and a phenyl linker ending in a carboxylic acid at the fourth *meso*  
13 position. The unfunctionalized dibenzophenazine explored in our studies is expected to  
14 foreshadow the properties of other dibenzophenazines derivatives to be the subject of future  
15 studies. Due to the vulnerability of dibenzophenazines to  $\pi$ - $\pi$  stacking, mesityl groups were  
16 appended to the tetrapyrrole core to prevent this via steric repulsion, thereby increasing solubility.  
17 The tetrapyrrole unit was selected for use in constructing an elongated  $\pi$ -conjugation system with  
18 the dibenzophenazines because of its ready structural flexibility and strong absorption profile  
19 which extends out to the red visible region. Tetrapyrroles also possess multiple available  
20 substitution positions that allowed our design described above, as well as the appendage of the  
21 anchoring carboxylic acid group, an essential component of many photosensitizers. The different  
22 structural configurations of our dyads (*ortho* versus *meta*) were prepared as a case study on the  
23 effects of substitution on panchromaticity; our DFT calculations indicated that while **PmZ** has a  
24 planar geometry as its minimum energy conformation, **PoZ**'s preferred conformation has a 23°  
25 dihedral angle between **Po** and the tetrapyrrole core for steric reasons (**Figure S6**). As the  
26 aggregation of photosensitizers is a known cause of low photovoltaic device efficiencies,<sup>44</sup> we  
27 explored whether the non-planarity of **PoZ** could result in overall better photosensitizing abilities  
28 than those of **PmZ**.  
29  
30  
31  
32  
33  
34  
35  
36  
37  
38  
39  
40  
41  
42  
43  
44  
45  
46  
47  
48  
49  
50  
51  
52  
53  
54  
55  
56  
57  
58  
59  
60

1  
2  
3 The syntheses of the phenazine-porphyrin dyads were based on palladium- and copper-catalyzed  
4 Sonogashira coupling of ethynyl phenazines and bromo porphyrins.<sup>82</sup> Our bromo porphyrin, **4**, is  
5 a *trans*-A<sub>2</sub>BC-porphyrin bearing two mesityl groups and a 4-carboxyphenyl group. Porphyrin **3**,  
6 the precursor porphyrin for all porphyrin derivatives discussed in this study, was prepared via a  
7 condensation reaction of dipyrromethane and mesitaldehyde in the presence of ethanol and  
8 BF<sub>3</sub>•OEt<sub>2</sub> followed by oxidation with DDQ.<sup>83</sup> The ethanol proved essential for a successful  
9 synthesis of the porphyrin.<sup>84</sup> **Scheme 2** shows the condensed syntheses of benchmark porphyrin  
10 **AZ**, and dyads **PmZ** and **PoZ**. The three steps required for generating **4** from **3** are described in  
11 the **Supporting Information**. They involve the selective bromination of **3** for the Suzuki coupling  
12 with methylbenzoate, followed by a bromination of **HZ** at the unsubstituted *meso* porphyrin site  
13 and zinc metalation with anhydrous zinc acetate to provide **4** in 91% yield. All porphyrins were  
14 preserved as esters until the final synthesis step in order to avoid unwanted side reactions.  
15  
16  
17  
18  
19  
20  
21  
22  
23  
24  
25  
26  
27  
28  
29

30 The syntheses of phenazines **Po** and **Pm** are described in **Scheme 1**, and the syntheses of  
31 diamines **1** and **2** are detailed in the **Supporting Information**. Our synthetic route deviates slightly  
32 from a reported procedure for the preparation of diethynylphenazines,<sup>48</sup> in that we couple  
33 ethynylbenzene-1,2-diamines bearing no protection groups with quinone derivatives. Condensation  
34 of phenanthrene-9,10-dione and ethynylbenzene-1,2-diamine in the presence of ethanol and  
35 dichloromethane afforded **Po** and **Pm** in 65% and 69% yields, respectively. The average yield for  
36 each synthetic step in the preparation of **Pm** was higher than the corresponding step of **Po**.  
37  
38  
39  
40  
41  
42  
43  
44  
45  
46  
47  
48  
49  
50  
51  
52  
53  
54  
55  
56  
57  
58  
59  
60

**Scheme 1. Syntheses of Ethynyldibenzophenazines**

Hydrolysis of the intermediate dyad esters with potassium hydroxide at room temperature afforded **PmZ** and **PoZ** in yields of 50% and 59%, respectively. Sonogashira coupling of ethynyltrimethylsilane and **4**, followed by a concurrent deprotection of trimethylsilyl (TMS) and hydrolysis in the presence of potassium hydroxide provided **AZ** in 69% yield.

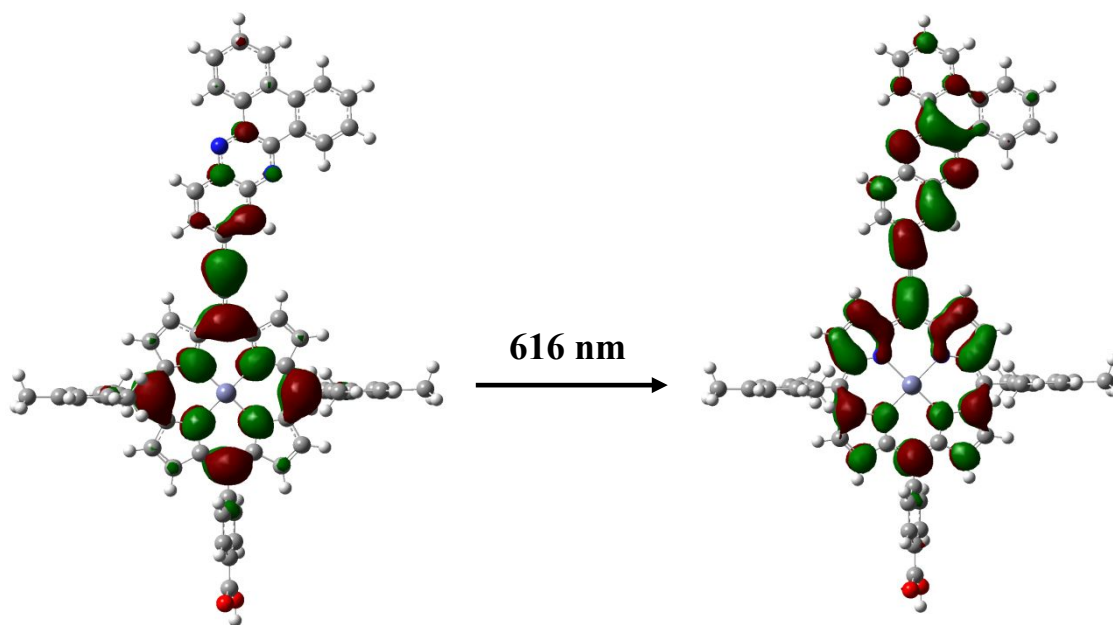
Scheme 2. Syntheses of Phenazine-Porphyrin Dyads<sup>a</sup>

<sup>a</sup> Reagents and conditions: **AZ**: Zn-bromoporphyrin (1 equiv), Pd(PPh<sub>3</sub>)<sub>2</sub>Cl<sub>2</sub> (25% mol), CuI (25% mol), trimethylsilylacetylene (20 equiv), triethylamine (30% of solvent), THF, -7 °C to room temp, 12 h. **PmZ** and **PoZ**: Zn-bromoporphyrin (1 equiv), ethynyl-dibenzophenazine (3 equiv), Pd<sub>2</sub>(dba)<sub>3</sub> (30% mol), CuI (5% mol), P(*o*-tol)<sub>3</sub> (2.4 equiv), triethylamine (20% of solvent), THF, 60 °C, overnight.

### Quantum Chemical Calculations.

Potential panchromatic dyad candidates for synthesis and experimental characterization were identified by using DFT calculations to obtain optimized molecular structures and simulated UV-Vis spectra. Examining the orbitals involved in the calculated transitions also provided a detailed

1  
2  
3 analysis of the origin of panchromaticity at the electronic level. In dyad systems with strong  
4 electronic coupling between the constituent chromophore units, desirable strong electronic  
5 transitions in the red (600–800 nm) region of the visible light spectrum resulted from the frontier  
6 orbitals of the system delocalized across the extended conjugated  $\pi$ -system of two dye moieties.  
7  
8  
9  
10  
11  
12 **Figure 2** and **Figure S5** underscore this point by showing natural transition orbital (NTO)  
13 projections for the relevant transitions in both **PmZ** and **PoZ**, respectively, showing that they  
14  
15 involve orbitals spanning the two moieties.  
16  
17  
18  
19



20  
21  
22  
23  
24  
25  
26  
27  
28  
29  
30  
31  
32  
33  
34  
35  
36  
37  
38  
39  
40  
41 **Figure 2.** Calculated transition at 616 nm for **PmZ** in its minimum-energy conformation.  
42  
43

44 Accordingly, where the goal is to design a dye that absorbs across a broad region of the solar  
45 spectrum, it is important to maximize the electronic interaction of the two dye components by  
46 making use of a fully-conjugating bridging group such as an ethynyl, as also demonstrated by other  
47 groups.<sup>85</sup> However, a variation in the degree of conjugation through the bridging group could tune  
48 the position of the red-most electronic transition. As a proof of principle, we evaluated five linker  
49 groups that connect phenazines with tetrapyrroles with varying degrees of conjugation, as well as  
50  
51  
52  
53  
54  
55  
56  
57  
58  
59  
60

their direct linkage. The DFT UV-Vis spectra of these species (**Figure 3**) show that the red-most absorption peak blueshifts and decreases in intensity as the conjugation between the two constituents decreases, from extensively conjugated ethynyl and vinyl linkers to weakly conjugated amidyl linkers. Because the ethynyl linker group offered the most promise for a panchromatic dye species, it was selected for use in synthesis and experimental characterization as described in the molecular design section.

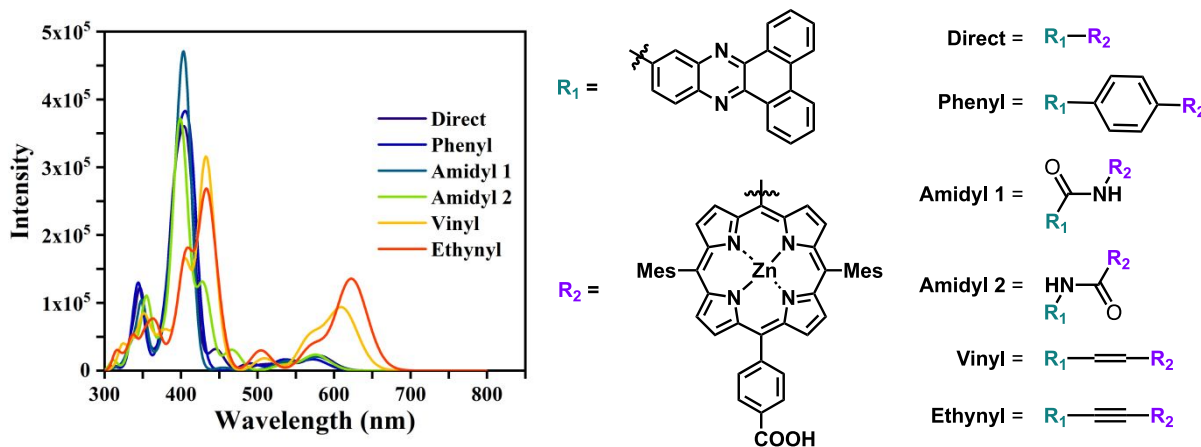
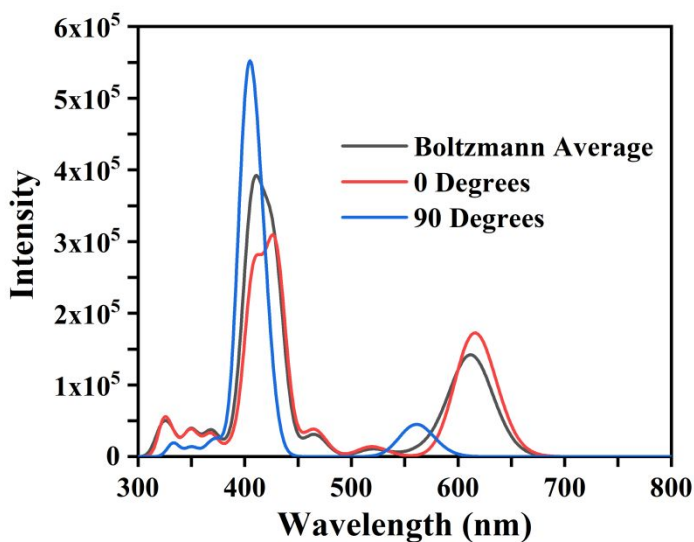


**Figure 3.** DFT calculated UV-Vis spectra of dyads with varying linkers in their minimum-energy conformations.

For dyad **PoZ**, the calculated minimum energy non-planar conformation involves a dihedral angle of 23 degrees between the phenazine and the tetrapyrrole. Because planarity is directly related to conjugation, it was initially assumed that **PoZ** would exhibit substantially less panchromaticity than **PmZ**. However, the ethynyl linker permits rotation, allowing the dihedral angles to vary without too great a loss of conjugation. Others have shown that it is important to take into account viable rotations when computing the absorption profile of dyes.<sup>86</sup> The rotational barriers of dyads **PmZ** and **PoZ** were calculated to be 1.35 kcal/mol and 1.70 kcal/mol, respectively (**Figure S2**). These relatively low barriers permit many conformations of these dyads

1  
2  
3 to contribute at room temperature under a Boltzmann distribution, influencing the average overall  
4 conjugation through the molecule and the UV-Vis spectra. Computing the UV-Vis spectra of these  
5 dyads in different conformations and combining them via their Boltzmann yields gives better  
6 relative intensities of the peaks. **Figure 4** shows simulated UV-Vis spectra with Boltzmann-  
7 averaged conformations for dyad **PmZ**. Similar results for **PoZ** and the calculated spectra of **HZ**  
8 and **AZ** can be found in the **Supporting Information (Figures S3 and S4)**. Notably, the rotation  
9 about the ethynyl triple bonds substantially reduces the intensity of the red-most visible electronic  
10 transition due to the contributions of less-conjugated conformations. This suggests that a similar  
11 dyad with full-conjugation and limited rotations could possess greater panchromatic absorption.  
12  
13  
14  
15  
16  
17  
18  
19  
20  
21  
22  
23  
24



25  
26  
27  
28  
29  
30  
31  
32  
33  
34  
35  
36  
37  
38  
39  
40  
41  
42  
43 **Figure 4.** DFT calculated UV-Vis spectra of **PmZ** in the planar minimum-energy conformation,  
44 with a 90 degree dihedral angle, and Boltzmann averaged across all rotational conformations.  
45  
46  
47  
48  
49

### 50 **Photophysical and Electrochemical Properties.**

51  
52 The electronic absorption spectra of phenazines **Po** and **Pm**, dyads **PmZ** and **PoZ**, as well as  
53 that of benchmark porphyrin **AZ** are shown in **Figure 5** with the data are tabulated in **Table 1**.  
54  
55  
56  
57  
58  
59  
60

1  
2  
3 The absorption spectrum of benchmark porphyrin **HZ** and emission spectra of **Po**, **Pm**, **AZ**, **PmZ**,  
4 and **PoZ** are displayed in the **Supporting Information (Figure S1)**. The overlaid spectra reveal  
5 that the absorption of **PmZ** and **PoZ** are not linear sums of those of the constituents **Pm**, **Pm**, **AZ**,  
6 and **HZ**; each exhibits new absorption peaks that are not observed for the constituents. The new  
7 peak at 640 nm is much more intense ( $\epsilon \sim 3.0 \times 10^4 \text{ M}^{-1}\cdot\text{cm}^{-1}$ ) and red-shifted relative to the  
8 Q-bands in the monomeric porphyrins ( $\lambda_{\text{abs}} \sim 610 \text{ nm}$ ,  $\epsilon \sim 0.50 \times 10^4 \text{ M}^{-1}\cdot\text{cm}^{-1}$ ) as a result of the  
9 conjugation of the phenazine and porphyrin derivatives. This underscores the existence and  
10 importance of strong electronic coupling between the two dyes through the ethynyl linker. Having  
11 a lower extinction coefficient but more similar intensities of the Soret and Q-bands, the phenazine-  
12 porphyrin dyad **PmZ** exhibits better orbital mixing and panchromaticity than **PoZ**. However, the  
13 wavelengths of the maximum absorptions and emissions are unaffected by the position of the  
14 ethynyl group (*ortho* versus *meta*) with respect to the zinc porphyrin, and the two dyads exhibit an  
15 almost identical absorption maximum wavelength in the red region. The integration of a phenazine  
16 moiety on one side of the molecule decreases the symmetry of the porphyrin macrocycle, resulting  
17 in less-degenerate  $B_x$  and  $B_y$  states and broader Soret bands in the porphyrin-phenazine dyads  
18 compared to those of the monomeric porphyrin **AZ**. The noncoplanar conformation of **PmZ**  
19 affords even less degenerate B states than in its counterpart **PoZ**, as shown by a larger spectral  
20 splitting in the Soret region. Importantly, both of the dyads demonstrate non-zero absorption from  
21 the near-ultraviolet to near-infrared regions (*i.e.* panchromatic absorption) which is apparent when  
22 compared to the absorption profile of the ethynylporphyrin **AZ**.  
23  
24  
25  
26  
27  
28  
29  
30  
31  
32  
33  
34  
35  
36  
37  
38  
39  
40  
41  
42  
43  
44  
45  
46  
47  
48  
49  
50  
51  
52  
53  
54  
55  
56  
57  
58  
59  
60

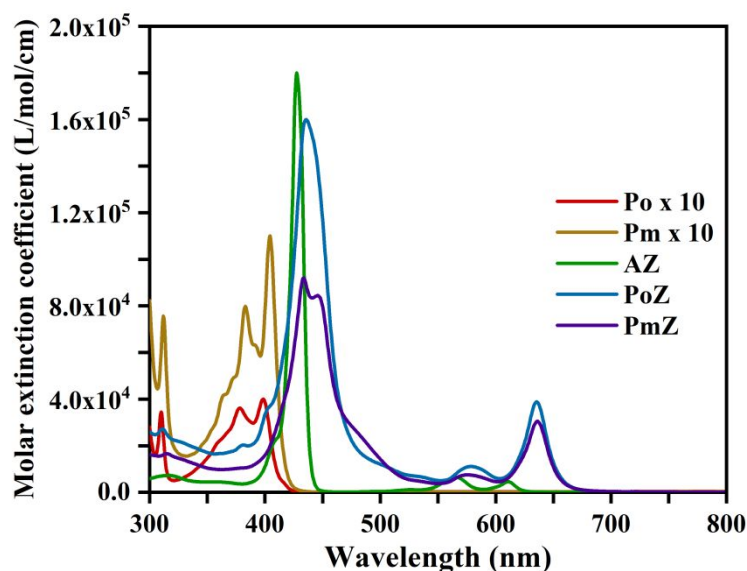


**Figure 5.** Absorption spectra of the of the phenazine and porphyrin derivatives **Po**, **Pm**, **AZ**, **PmZ** and **PoZ** collected in anhydrous methanol and toluene, respectively, at room temperature. The molar extinction coefficients of the phenazine **Po** and **Pm** are amplified ten times in intensity for clear comparison. The emission spectra were recorded with excitation wavelengths noted in **Table S2**.

**Table 1.** Absorption Features of the Dyads and Benchmark Compounds.

| Compound   | $\lambda_{\text{abs}}$ (nm) <sup>a</sup> | $\epsilon_{\text{max}}$ ( $\times 10^5 \text{ M}^{-1} \cdot \text{cm}^{-1}$ ) <sup>b</sup> | $\text{FWHM}_{\text{Soret}}$ ( $\text{cm}^{-1}$ ) <sup>c</sup> |
|------------|--|--|--|
| <b>PmZ</b> | 434, 446, 576, 636                       | 0.92   | 2018   |
| <b>PoZ</b> | 434, 578, 636                            | 1.6  | 1743   |
| <b>AZ</b>  | 428, 566, 611                            | 1.8  | 655  |
| <b>Pm</b>  | 312, 383, 404                            | 0.11   | —  |
| <b>Po</b>  | 310, 378, 398                            | 0.040  | —  |

1  
2  
3 <sup>a</sup>Absorption spectra and molar absorption coefficients were measured in methanol at room  
4 temperature with absorbance around 1. <sup>b</sup>Molar absorption coefficient of the peak with the  
5 maximum absorbance. <sup>c</sup>Full width at half maximum of Soret bands of porphyrins.  
6  
7  
8  
9

10  
11  
12 The molecular structures of **PmZ-Ester**, **PoZ-Ester**, and **AZ-Ester**, which are ester versions of  
13 the **PmZ**, **PoZ**, and **AZ**, are shown in the **Supporting Information**, as well as the cyclic  
14 voltammogram (CV) of **HZ-Ester**. As seen in **Figure 6**, the CVs of **AZ-Ester** and **PoZ-Ester**  
15 exhibit pronounced irreversibility of the first oxidation feature while **PmZ-Ester** exhibits only  
16 mild irreversibility of this same feature. The loss of the return feature suggests that a chemical  
17 change may be taking place upon oxidation, likely involving the ethynyl group. Ethynyl groups  
18 have high acidity and reactivity, which are further increased under these oxidizing conditions.<sup>85</sup>  
19 The increased reversibility of **PmZ-Ester** as compared to **PoZ-Ester** could in part be explained  
20 by the structure and conjugation of the molecules. The minimum energy conformation of **PoZ-**  
21 **Ester** is non-planar with a dihedral angle of 23 degrees; however, it is completely planar for **PmZ-**  
22 **Ester**. This causes the ethynyl group of **PoZ-Ester** to be more similar to that of **AZ-Ester** and,  
23 therefore, more susceptible to a chemical reaction. **PmZ-Ester**, alternatively, has a minimum  
24 energy conformation with increased conjugation between the porphyrin and the phenazine due to  
25 its planarity, shifting the electronic properties of the ethynyl group. To probe when the chemical  
26 change may take place, the potential window was narrowed to 1.25 V vs NHE, but the  
27 irreversibility remained. This indicates that if a chemical change does occur, it happens at or near  
28 the potential of the first oxidation feature.  
29  
30  
31  
32  
33  
34  
35  
36  
37  
38  
39  
40  
41  
42  
43  
44  
45  
46  
47  
48  
49  
50  
51  
52  
53  
54  
55  
56  
57  
58  
59  
60

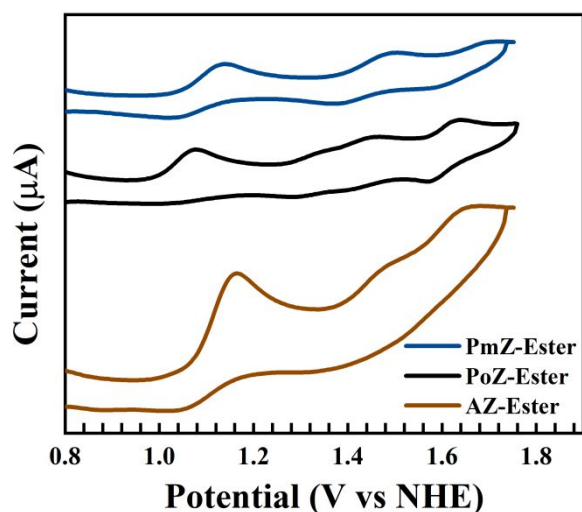


**Figure 6.** Cyclic voltammograms of **AZ-Ester**, **PoZ-Ester**, and **PmZ-Ester** in 0.1 M TBAPF<sub>6</sub> in dichloromethane with a 50 mV/s scan rate.

### Photovoltaic Performance.

The performance of TiO<sub>2</sub>-based photovoltaic devices with photosensitizers **HZ**, **AZ**, **PmZ** and **PoZ** were measured under standard conditions (AM 1.5G, 100 mW/cm<sup>2</sup>) using iodine/triiodide (I<sup>-</sup>/I<sub>3</sub><sup>-</sup>) liquid electrolyte. Additional photovoltaic parameters are summarized in **Table 2**; MK-2 was used as a reference cell and its overall efficiency of  $4.97 \pm 0.25$  agreed closely with the literature.<sup>87</sup> The phenazine-porphyrin dyads **PoZ** and **PmZ** perform better than the benchmark porphyrins **HZ** and **AZ** as expected given their panchromatic absorption (**Figure 7**). Of the two dyads, **PmZ** performed the best, affording an open-circuit photovoltage ( $V_{oc}$ ) of 0.61 V, a short-circuit photocurrent density ( $J_{sc}$ ) of 5.47 mA/cm<sup>2</sup>, a fill factor (ff) of 0.68, and an overall solar-to-electrical energy conversion efficiency ( $\eta$ ) of 2.29%. Additionally, the device with **PmZ** exhibited a higher surface coverage of dye molecules, which could be a result of the increased planarity of **PmZ**, allowing more photosensitizers access to the TiO<sub>2</sub> surface. While performing other optimizations of the devices would likely improve their efficiencies, the focus of this study is on

the electronic and photophysical properties of the dyes, not on the optimization of photovoltaic devices.

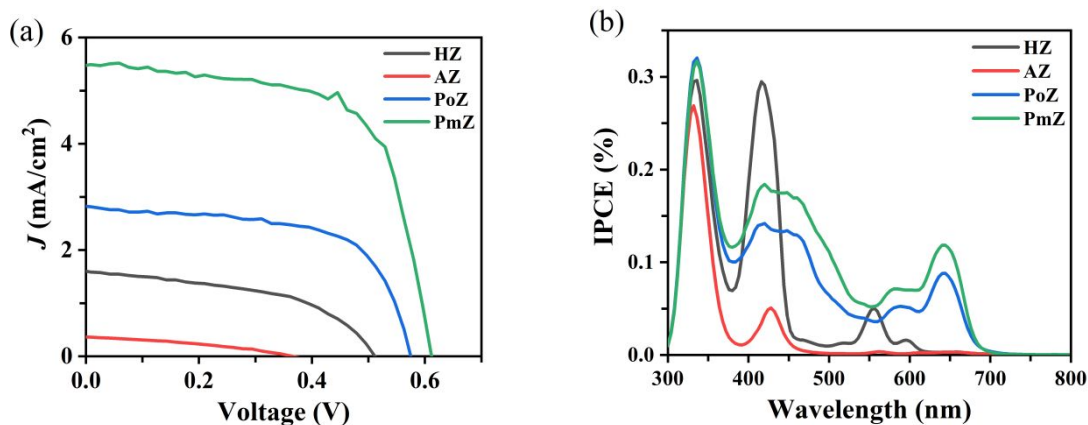


**Figure 7.** (a) current density vs. voltage ( $J$ - $V$ ) curve and (b) incident photon to current efficiency (IPCE) profile of devices with photosensitizers **HZ**, **AZ**, **PoZ**, and **PmZ**.

**Table 2.** Photovoltaic Parameters for photosensitizers **HZ**, **AZ**, **PoZ**, and **PmZ**.

| cell specification | $V_{oc}$ (V)    | $J_{sc}$ (mA/cm <sup>2</sup> ) | ff (%)          | $\eta$ (%)      | dye surface coverage (mM/cm <sup>2</sup> ) | $\eta$ (%) / dye surface coverage |
|--------------------|-----------------|--------------------------------|-----------------|-----------------|--|-----------------------------------|
| <b>HZ</b>          | $0.52 \pm 0.02$ | $1.60 \pm 0.22$                | $0.56 \pm 0.08$ | $0.47 \pm 0.12$ | 0.037                                      | 12.7                              |
| <b>AZ</b>          | $0.39 \pm 0.05$ | $0.36 \pm 0.09$                | $0.40 \pm 0.19$ | $0.06 \pm 0.05$ | 0.024                                      | 2.5                               |
| <b>PoZ</b>         | $0.57 \pm 0.01$ | $2.58 \pm 0.49$                | $0.63 \pm 0.06$ | $0.94 \pm 0.19$ | 0.039                                      | 24.1                              |
| <b>PmZ</b>         | $0.61 \pm 0.01$ | $5.47 \pm 0.60$                | $0.68 \pm 0.02$ | $2.29 \pm 0.27$ | 0.074                                      | 31.0                              |

## Conclusions

We have prepared two bichromophoric phenazine-porphyrin dyads and evaluated their photophysical, electrochemical, and photovoltaic properties. We pre-determined the structures of

1  
2  
3 the dyads with suitable absorption profiles from quantum chemistry calculations. Calculations of  
4 the absorption spectra of dibenzophenazine connected to a tetrapyrrole with a variety of linkers  
5 showed that the ethynyl linker gave the broadest absorption coverage because of the stronger  
6 electronic coupling between the two constituent dyes. The dyads, synthesized via a Sonogashira  
7 coupling of ethynyl phenazines and bromo-porphyrins, showed absorption extending from 300 nm  
8 to 636 nm. The reported results demonstrate that the conjugated linkage of phenazines and  
9 tetrapyrroles yields panchromatic absorption, paving the way for the rational design of improved  
10 panchromatic dyads.  
11  
12  
13  
14  
15  
16  
17  
18  
19  
20  
21  
22  
23

## 24 ■ **Experimental Section**

### 25 **Synthesis.**

26 The syntheses of molecules are described in the **Supporting Information**.  
27  
28

### 29 **Absorption and Emission.**

30 UV-visible spectrophotometry was performed using a Shimadzu UV-2600 spectrophotometer  
31 coupled with UVProbe software. Sample solutions were carried in 1 cm x 1 cm quartz cuvettes to  
32 measure the steady-state absorption spectra and molar extinction coefficients. A detailed procedure  
33 for measuring molar extinction coefficients is described in the **Supporting Information**.  
34  
35  
36  
37  
38  
39  
40  
41

### 42 **Electrochemistry.**

43 Cyclic Voltammetry (CV) experiments were conducted using a Pine WaveNow potentiostat. A  
44 glassy carbon working electrode, a Ag/AgCl wire pseudoreference electrode and a platinum wire  
45 counter electrode made up the three-electrode electrochemical cell. The glassy carbon working  
46 electrode was polished with an alumina slurry on a polishing pad before each experiment. The  
47 supporting electrolyte was 0.1 M tetrabutylammonium hexafluorophosphate (TBAPF<sub>6</sub>),  
48  
49  
50  
51  
52  
53  
54  
55  
56  
57  
58  
59  
60

1  
2  
3 recrystallized twice prior to use, in anhydrous dichloromethane. To establish the potential of the  
4 pseudoreference electrode, the ferrocenium/ferrocene redox couple was used as an internal  
5 standard. All CVs were referenced to NHE using the measured ferrocenium/ferrocene  $E_{1/2}$  which  
6 is 0.690 V vs NHE in dichloromethane.<sup>88</sup> Reported CVs were performed in an electrochemical cell  
7 that had been purged with  $N_2$ , but no difference was seen in the CVs recorded under air. The  
8 porphyrin concentration was 1 mM, and a 50 mV/s scan rate was used for each reported CV.  
9  
10  
11  
12  
13  
14  
15  
16

### 17 **Dye-Sensitized Solar Cell (DSSC) Fabrication and Photovoltaic Measurements.**

18  
19 The DSSCs were fabricated according to the previously reported methods and the details are  
20 described in the **Supporting Information**.<sup>87</sup> The current density-voltage ( $J$ - $V$ ) and incident photo-  
21 to-electron conversion efficiency (IPCE) data were measured using a PARSTAT 4000 potentiostat  
22 (Princeton Applied Research) and a solar simulator equipped with a 1000 W ozone-free Xenon  
23 lamp and AM1.5G filter. The light intensity was calibrated with ASTM E948-09 and E1021-06  
24 standards (Newport). Spectra of the monochromatic IPCEs for the solar cells were obtained using  
25 a Keithley 2400 source meter and custom LabView software developed by our group. The dye-  
26 loadings were measured by soaking each slide in a solution of 0.05 M NaOH in  
27 water/tetrahydrofuran/ethanol (v/v/v, 1:1:1) for 4 days, drying via rotatory evaporation, and  
28 measuring their absorption spectra in methanol. The concentrations of the solutions were  
29 calculated with experimentally determined molar extinction coefficients.  
30  
31  
32  
33  
34  
35  
36  
37  
38  
39  
40  
41  
42  
43

### 44 **DFT Calculations.**

45  
46 All structures studied in this manuscript were optimized using DFT at the B3LYP<sup>89</sup>/def2SVP<sup>90</sup>  
47 level using the Gaussian09 software package.<sup>91</sup> Frequency calculations verified that the obtained  
48 minimum energy geometry was a stationary point. Linear-response time-dependent DFT  
49 calculations<sup>92</sup> were performed with an implicit methanol polarizable continuum model<sup>93</sup> to obtain  
50  
51  
52  
53  
54  
55  
56  
57  
58  
59  
60

1  
2  
3 the forty-five lowest-energy singlet electronic transitions for each molecule. Spectra shown in the  
4 manuscript were subjected to a 0.075 eV Gaussian broadening to better match experimentally  
5 obtained spectra. Rotation barrier calculations were performed by fixing the dihedral angle  
6 between the two dyes in increments of 5 degrees from 0 to 90 degrees and relaxing the rest of the  
7 structure. Conformationally averaged calculated spectra were obtained by weighting the  
8 calculated spectra of each rotamer by the Boltzmann weight determined by its electronic energy  
9 relative to the minimum-energy conformation and then normalizing to 1. Natural Transition  
10 Orbital<sup>94</sup> Analysis was used to visualize select calculated transitions as a single pair of orbitals, an  
11 excited 'particle' and an empty 'hole'.  
12  
13  
14  
15  
16  
17  
18  
19  
20  
21  
22  
23  
24  
25

## 26 ASSOCIATED CONTENT

### 27 28 29 **Supporting Information.**

30  
31  
32 This information can be found online at The Supporting Information for free of charge on the  
33 ACS Publications website at DOI:  
34  
35

36  
37  
38 Synthesis and characterization of the dyads, additional absorption and emission spectra, CV data,  
39 and details on quantum calculation results (PDF).  
40  
41  
42  
43

### 44 **Corresponding Authors**

45  
46 \* To whom correspondence should be addressed:

47  
48 Phone: 203-200-8936      [robert.crabtree@yale.edu](mailto:robert.crabtree@yale.edu)

49  
50 Phone: 203-432-6672      [victor.batista@yale.edu](mailto:victor.batista@yale.edu)

51  
52 Phone: 203-432-5202      [gary.brudvig@yale.edu](mailto:gary.brudvig@yale.edu)  
53  
54  
55  
56  
57  
58  
59  
60

1  
2  
3  
4  
5  
6 **Author Contributions**  
7

8 ‡These authors contributed equally.  
9

10  
11 **ACKNOWLEDGMENT**  
12

13  
14 We thank the staff at Yale West Campus Analytical Core, Yale Chemical and Biophysical  
15 Instrumentation Center for their help with the instrumentations. This work was supported by the  
16 U.S. Department of Energy, Chemical Sciences, Geosciences, and Biosciences Division, Office of  
17 Basic Energy Sciences, Office of Science (Grant DEFG02-07ER15909). Additional support was  
18 provided by a generous donation from the TomKat Charitable Trust. V.S.B. acknowledges  
19 computational time from NERSC and Yale HPC. A.J.M. was supported by the National Science  
20 Foundation Graduate Research Fellowship under Grant No. DGE-1122492.  
21  
22  
23  
24  
25  
26  
27  
28  
29  
30  
31  
32  
33  
34  
35  
36  
37  
38  
39  
40  
41  
42  
43  
44  
45  
46  
47  
48  
49  
50  
51  
52  
53  
54  
55  
56  
57  
58  
59  
60

## REFERENCES

1. Listorti, A.; Durrant, J.; Barber, J. Artificial Photosynthesis: Solar to Fuel. *Nat. Mater.* **2009**, *8*, 929–930.
2. Scholes, G. D.; Fleming, G. R.; Olaya-Castro, A.; van Grondelle, R. Lessons from Nature about Solar Light Harvesting. *Nat. Chem.* **2011**, *3*, 763–774.
3. Frischmann, P. D.; Mahata, K.; Würthner, F. Powering the Future of Molecular Artificial Photosynthesis with Light-Harvesting Metallo-supramolecular Dye Assemblies. *Chem. Soc. Rev.* **2013**, *42*, 1847–1870.
4. Berardi, S.; Drouet, S.; Francàs, L.; Gimbert-Suriñach, C.; Guttentag, M.; Richmond, C.; Stoll, T.; Llobet, A. Molecular Artificial Photosynthesis. *Chem. Soc. Rev.* **2014**, *43*, 7501–7519.
5. Sekine, K.; Stuck, F.; Schulmeister, J.; Wurm, T.; Zetschok, D.; Rominger, F.; Rudolph, M.; Hashmi, A. S. K. N-Heterocycle-Fused Pentalenones by a Gold-Catalyzed Annulation of Diethynyl-Quinoxalines and -Phenazines. *Chem. Eur. J.* **2018**, *24*, 12515–12518.
6. Barber, J. Photosystem II: a Multisubunit Membrane Protein that Oxidises Water. *Curr. Opin. Struct. Biol.* **2002**, *12*, 523–530.
7. Polívka, T.; Sundström, V. Ultrafast Dynamics of Carotenoid Excited State—From Solution to Natural and Artificial Systems. *Chem. Rev.* **2004**, *104*, 2021–2071.
8. Müh, F.; Madjet, M. E.-A.; Adolphs, J.; Abdurahman, A.; Rabenstein, B.; Ishikita, H.; Knapp, E.-W.; Renger, T.  $\alpha$ -Helices Direct Excitation Energy Flow in the Fenna–Matthews–Olson Protein. *Proc. Natl. Acad. Sci. U. S. A.* **2007**, *104*, 16862–16867.
9. Adolphs, J.; Müh, F.; Madjet, M. E.-A.; Renger, T. Calculation of Pigment Transition Energies in the FMO Protein: From Simplicity to Complexity and Back. *Photosynth. Res.* **2008**, *95*, 197–209.
10. am Busch, M. S.; Müh, F.; Madjet, M. E.-A.; Renger, T. The Eighth Bacteriochlorophyll Completes the Excitation Energy Funnel in the FMO Protein. *J. Phys. Chem. Lett.* **2011**, *2*, 93–98.
11. Moore, G. F.; Brudvig, G. W. Energy Conversion in Photosynthesis: A Paradigm for Solar Fuel Production. *Annu. Rev. Condens. Matter Phys.* **2011**, *2*, 303–327.
12. Hildner, R.; Brinks, D.; Nieder, J. B.; Cogdell, R. J.; van Hulst, N. F. Quantum Coherent Energy Transfer over Varying Pathways in Single Light-Harvesting Complexes. *Science* **2013**, *340*, 1448–1451.
13. Liu, Y.; Lin, H.; Li, X.; Li, J.; Nan, H. Photoinduced Electron Transfer in Panchromatic Zinc Phthalocyanine–Azobenzene Dyad. *Inorg. Chem. Commun.* **2010**, *13*, 187–190.
14. Rio, Y.; Seitz, W.; Gouloumis, A.; Vázquez, P.; Sessler, J. L.; Guldi, D. M.; Torres, T. A Panchromatic Supramolecular Fullerene-Based Donor–Acceptor Assembly Derived from a Peripherally Substituted Bodipy–Zinc Phthalocyanine Dyad. *Chem. Eur. J.* **2010**, *16*, 1929–1940.

15. Warnan, J.; Buchet, F.; Pellegrin, Y.; Blart, E.; Odobel, F. Panchromatic Trichromophoric Sensitizer for Dye-Sensitized Solar Cells Using Antenna Effect. *Org. Lett.* **2011**, *13*, 3944–3947.
16. Bozdemir, O. A.; Erbas-Cakmak, S.; Ekiz, O. O.; Dana, A.; Akkaya, E. U. Towards Unimolecular Luminescent Solar Concentrators: Bodipy-Based Dendritic Energy-Transfer Cascade with Panchromatic Absorption and Monochromatized Emission. *Angew. Chem. Int. Ed.* **2011**, *50*, 10907–10912.
17. Bartelmess, J.; Soares, A. R. M.; Martínez-Díaz, M. V.; Neves, M. G. P. M. S.; Tomé, A. C.; Cavaleiro, J. A. S.; Torres, T.; Guldi, D. M. Panchromatic Light Harvesting in Single Wall Carbon Nanotube Hybrids—Immobilization of Porphyrin–Phthalocyanine Conjugates. *Chem. Commun.* **2011**, *47*, 3490–3492.
18. Nieto, C. R.; Guilleme, J.; Villegas, C.; Delgado, J. L.; González-Rodríguez, D.; Martín, N.; Torres, T.; Guldi, D. M., Subphthalocyanine-Polymethine Cyanine Conjugate: an All Organic Panchromatic Light Harvester that Reveals Charge Transfer. *J. Mater. Chem. A* **2011**, *21*, 15914–15918.
19. Warnan, J.; Gardner, J.; Le Pleux, L.; Petersson, J.; Pellegrin, Y.; Blart, E.; Hammarström, L.; Odobel, F. Multichromophoric Sensitizers Based on Squaraine for NiO Based Dye-Sensitized Solar Cells. *J. Phys. Chem. C* **2014**, *118*, 103–113.
20. M'Sabah, B. L.; Boucharef, M.; Warnan, J.; Pellegrin, Y.; Blart, E.; Lucas, B.; Odobel, F.; Bouclé, J. Amplification of Light Collection in Solid-State Dye-Sensitized Solar Cells *via* the Antenna Effect Through Supramolecular Assembly. *Phys. Chem. Chem. Phys.* **2015**, *17*, 9910–9918.
21. Jradi, F. M.; O'Neil, D.; Kang, X.; Wong, J.; Szymanski, P.; Parker, T. C.; Anderson, H. L.; El-Sayed, M. A.; Marder, S. R. A Step Toward Efficient Panchromatic Multi-Chromophoric Sensitizers for Dye Sensitized Solar Cells. *Chem. Mater.* **2015**, *27*, 6305–6313.
22. Lebedeva, M. A.; Chamberlain, T. W.; Scattergood, P. A.; Delor, M.; Sazanovich, I. V.; Davies, E. S.; Suyetin, M.; Besley, E.; Schröder, M.; Weinstein, J. A.; Khlobystov, A. N. Stabilising the Lowest Energy Charge-Separated State in a {Metal Chromophore – Fullerene} Assembly: a Tuneable Panchromatic Absorbing Donor–Acceptor Triad. *Chem. Sci.* **2016**, *7*, 5908–5921.
23. Hu, G.; Liu, R.; Alexy, E. J.; Mandal, A. K.; Bocian, D. F.; Holten, D.; Lindsey, J. S. Panchromatic Chromophore–Tetrapyrrole Light-Harvesting Arrays Constructed from Bodipy, Perylene, Terrylene, Porphyrin, Chlorin, and Bacteriochlorin Building Blocks. *New J. Chem.* **2016**, *40*, 8032–8052.
24. Sekita, M.; Ballesteros, B.; Diederich, F.; Guldi, D. M.; Bottari, G.; Torres, T. Intense Ground-State Charge Transfer Interactions in Low-Bandgap, Panchromatic Phthalocyanine–Tetracyanobuta-1,3-diene Conjugates. *Angew. Chem. Int. Ed.* **2016**, *55*, 5560–5564.
25. Mishra, R.; Regar, R.; Singhal, R.; Panini, P.; Sharma, G. D.; Sankar, J. Porphyrin Based Push–Pull Conjugates as Donors for Solution-Processed Bulk Heterojunction Solar Cells:

- a Case of Metal-Dependent Power Conversion Efficiency. *J. Mater. Chem. A* **2017**, *5*, 15529–15533.
26. Tsai, M.-C.; Wang, C.-L.; Chang, C.-W.; Hsu, C.-W.; Hsiao, Y.-H.; Liu, C.-L.; Wang, C.-C.; Lin, S.-Y.; Lin, C.-Y. A Large, Ultra-Black, Efficient and Cost-Effective Dye-Sensitized Solar Module Approaching 12% Overall Efficiency under 1000 lux Indoor Light. *J. Mater. Chem. A* **2018**, *6*, 1995–2003.
27. Fernández-Ariza, J.; Urbani, M.; Rodríguez-Morgade, M. S.; Torres, T. Panchromatic Photosensitizers Based on Push–Pull, Unsymmetrically Substituted Porphyrazines. *Chem. Eur. J.* **2018**, *24*, 2618–2625.
28. Kawata, T.; Chino, Y.; Kobayashi, N.; Kimura, M. Increased Light-Harvesting in Dye-Sensitized Solar Cells through Förster Resonance Energy Transfer within Supramolecular Dyad Systems. *Langmuir* **2018**, *34*, 7294–7300.
29. Aumaitre, C.; Rodriguez-Seco, C.; Jover, J.; Bardagot, O.; Caffy, F.; Kervella, Y.; López, N.; Palomares, E.; Demadrille, R. Visible and Near-Infrared Organic Photosensitizers Comprising Isoindigo Derivatives as Chromophores: Synthesis, Optoelectronic Properties and Factors Limiting their Efficiency in Dye Solar Cells. *J. Mater. Chem. A* **2018**, *6*, 10074–10084.
30. Desta, M. B.; Vinh, N. S.; Kumar, CH. P.; Chaurasia, S.; Wu, W.-T.; Lin, J. T.; Wei, T.-C.; Diao, E. W.-G. Pyrazine-Incorporating Panchromatic Sensitizers for Dye Sensitized Solar Cells under One Sun and Dim Light. *J. Mater. Chem. A* **2018**, *6*, 13778–13789.
31. Kabir, E.; Patel, D.; Clark, K.; Teets, T. S. Spectroscopic and Electrochemical Properties of Electronically Modified Cycloplatinated Formazanate Complexes. *Inorg. Chem.* **2018**, *57*, 10906–10917.
32. Yuen, J. M.; Diers, J. R.; Alexy, E. J.; Roy, A.; Mandal, A. K.; Kang, H. S.; Niedzwiedzki, D. M.; Kirmaier, C.; Lindsey, J. S.; Bocian, D. F.; Holten, D. Origin of Panchromaticity in Multichromophore–Tetrapyrrole Arrays. *J. Phys. Chem. A* **2018**, *122*, 7181–7201.
33. Liao, J.; Zhao, H.; Cai, Z.; Xu, Y.; Qin, F. G. F.; Zong, Q.; Peng, F.; Fang, Y. BODIPY-Based Panchromatic Chromophore for Efficient Organic Solar Cell. *Org. Electron.* **2018**, *61*, 215–222.
34. Ho, P.-Y.; Mark, M. F.; Wang, Y.; Yiu, S.-C.; Yu, W.-H.; Ho, C.-L.; McCamant, D. W.; Eisenberg, R.; Huang, S. Panchromatic Sensitization with Zn<sup>II</sup> Porphyrin-Based Photosensitizers for Light-Driven Hydrogen Production. *ChemSusChem* **2018**, *11*, 2517–2528.
35. Urbani, M.; Grätzel, M.; Nazeeruddin, M. K.; Torres, T. Meso-Substituted Porphyrins for Dye-Sensitized Solar Cells. *Chem. Rev.* **2014**, *114*, 12330–12396.
36. He, B.; Zhrebetsky, D.; Wang, H.; Kolaczowski, M. A.; Klivansky, L. M.; Tan, T.; Wang, L.; Liu, Y. Rational Tuning of High-Energy Visible Light Absorption for Panchromatic Small Molecules by a Two-Dimensional Conjugation Approach. *Chem. Sci.* **2016**, *7*, 3857–3861.

- 1  
2  
3 37. Lin, V. S.-Y.; DiMagno, S. G.; Therien, M. J. Highly Conjugated, Acetylenyl Bridged  
4 Porphyrins: New Models for Light-Harvesting Antenna Systems. *Science* **1994**, *264*,  
5 1105–1111.  
6  
7 38. Imahori, H.; Matsubara, Y.; Iijima, H.; Umeyama, T.; Matano, Y.; Ito, S.; Niemi, M.;  
8 Tkachenko, N. V.; Lemmetyinen, H. Effects of *meso*-Diaryl amino Group of Porphyrins as  
9 Sensitizers in Dye-Sensitized Solar Cells on Optical, Electrochemical, and Photovoltaic  
10 Properties. *J. Phys. Chem. C* **2010**, *114*, 10656–10665.  
11  
12 39. Ragoussi, M.-E.; de la Torre, G.; Torres, T. Tuning the Electronic Properties of Porphyrin  
13 Dyes: Effects of *meso* Substitution on Their Optical and Electrochemical Behaviour. *Eur.*  
14 *J. Org. Chem.* **2013**, 2832–2840.  
15  
16 40. Alexy, E. J.; Yuen, J. M.; Chandrashaker, V.; Diers, J. R.; Kirmaier, C.; Bocian, D. F.;  
17 Holten, D.; Lindsey, J. S. Panchromatic Absorbers for Solar Light-Harvesting. *Chem.*  
18 *Commun.* **2014**, 50, 14512–14515.  
19  
20 41. Tanaka, T.; Osuka, A. Conjugated Porphyrin Arrays: Synthesis, Properties and  
21 Applications for Functional Materials. *Chem. Soc. Rev.* **2015**, *44*, 943–969.  
22  
23 42. Mandal, A. K.; Diers, J. R.; Niedzwiedzki, D. M.; Hu, G.; Liu, R.; Alexy, E. J.; Lindsey,  
24 J. S.; Bocian, D. F.; Holten, D. Tailoring Panchromatic Absorption and Excited-State  
25 Dynamics of Tetrapyrrole–Chromophore (Bodipy, Rylene) Arrays—Interplay of Orbital  
26 Mixing and Configuration Interaction. *J. Am. Chem. Soc.* **2017**, *139*, 17547–17564.  
27  
28 43. Cheema, H.; Peddapuram, A.; Adams, R. E.; McNamara, L.; Hunt, L. A.; Le, N.; Watkins,  
29 D. L.; Hammer, N. I.; Schmehl, R. H.; Delcamp, J. H. Molecular Engineering of Near  
30 Infrared Absorbing Thienopyrazine Double Donor Double Acceptor Organic Dyes for  
31 Dye-Sensitized Solar Cells. *J. Org. Chem.* **2017**, *82*, 12038–12049.  
32  
33 44. Hu, G.; Kang, H. S.; Mandal, A. K.; Roy, A.; Kirmaier, C.; Bocian, D. F.; Holten, D.;  
34 Lindsey, J. S. Synthesis of Arrays Containing Porphyrin, Chlorin, and Perylene-Imide  
35 Constituents for Panchromatic Light-Harvesting and Charge Separation. *RSC Adv.* **2018**,  
36 *8*, 23854–23874.  
37  
38 45. Spicer, J. A.; Gamage, S. A.; Rewcastle, G. W.; Finlay, G. J.; Bridewell, D. J. A.; Baguley,  
39 B. C.; Denny, W. A. Bis(phenazine-1-carboxamides): Structure–Activity Relationships for  
40 a New Class of Dual Topoisomerase I/II-Directed Anticancer Drugs. *J. Med. Chem.* **2000**,  
41 *43*, 1350–1358.  
42  
43 46. Vicker, N.; Burgess, L.; Chuckowree, I. S.; Dodd, R.; Folkes, A. J.; Hardick, D. J.; Hancox,  
44 T. C.; Miller, W.; Milton, J.; Sohal, S.; Wang, S.; Wren, S. P.; Charlton, P. A.; Dangerfield,  
45 W.; Liddle, C.; Mistry, P.; Stewart, A. J.; Denny, W. A. Novel Angular Benzophenazines:  
46 Dual Topoisomerase I and Topoisomerase II Inhibitors as Potential Anticancer Agents. *J.*  
47 *Med. Chem.* **2002**, *45*, 721–739.  
48  
49 47. Bunz, U. H. F. N-Heteroacenes. *Chem. Eur. J.* **2009**, *15*, 6780–6789.  
50  
51 48. Bryant, J. J.; Zhang, Y.; Lindner, B. D.; Davey, E. A.; Appleton, A. L.; Qian, X.; Bunz, U.  
52 H. F. Alkynylated Phenazines: Synthesis, Characterization, and Metal-Binding Properties  
53 of Their Bis-Triazolyl Cycloadducts. *J. Org. Chem.* **2012**, *77*, 7479–7486.  
54  
55  
56  
57  
58  
59  
60

- 1  
2  
3 49. Bunz, U. H. F.; Engelhart, J. U.; Lindner, B. D.; Schaffroth, M. Large N-Heteroacenes:  
4 New Tricks for Very Old Dogs? *Angew. Chem. Int. Ed.* **2013**, *52*, 3810–3821.  
5  
6 50. Gu, P.-Y.; Zhao, Y.; He, J.-H.; Zhang, J.; Wang, C.; Xu, Q.-F.; Lu, J.-M.; Sun, X. W.;  
7 Zhang, Q. Synthesis, Physical Properties, and Light-Emitting Diode Performance of  
8 Phenazine-Based Derivatives with Three, Five, and Nine Fused Six-Membered Rings. *J.*  
9 *Org. Chem.* **2015**, *80*, 3030–3035.  
10  
11 51. Koepf, M.; Lee, S. H.; Brennan, B. J.; Méndez-Hernández, D. D.; Batista, V. S.; Brudvig,  
12 G. W.; Crabtree, R. H. Preparation of Halogenated Fluorescent Diaminophenazine  
13 Building Blocks. *J. Org. Chem.* **2015**, *80*, 9881–9888.  
14  
15 52. Lorenz, R.; Kaifer, E.; Wadepohl, H.; Himmel, H.-J. Di- and Tetranuclear Transition Metal  
16 Complexes of a Tetrakisguanidino-Substituted Phenazine Dye by Stepwise Coordination.  
17 *Dalton Trans.* **2018**, *47*, 11016–11029.  
18  
19 53. Sheng, J.; He, R.; Xue, J.; Wu, C.; Qiao, J.; Chen, C. Cu-Catalyzed  $\pi$ -Core Evolution of  
20 Benzoxadiazoles with Diaryliodonium Salts for Regioselective Synthesis of Phenazine  
21 Scaffolds. *Org. Lett.* **2018**, *20*, 4458–4461.  
22  
23 54. Seillan, C.; Brisset, H.; Siri, O. Efficient Synthesis of Substituted  
24 Dihydropyridopyrimidines. *Org. Lett.* **2008**, *10*, 4013–4016.  
25  
26 55. Rewcastle, G. W.; Denny, W. A.; Baguley, B. C. Potential Antitumor Agents. 51. Synthesis  
27 and Antitumor Activity of Substituted Phenazine-1-carboxamides. *J. Med. Chem.* **1987**,  
28 *30*, 843–851.  
29  
30 56. Price-Whelan, A.; Dietrich, L. E. P.; Newman, D. K. Rethinking 'Secondary' Metabolism:  
31 Physiological Roles for Phenazine Antibiotics. *Nat. Chem. Biol.* **2006**, *2*, 71–78.  
32  
33 57. Rohrabough, T. N., Jr.; Collins, K. A.; Xue, C.; White, J. K.; Kodanko, J. J.; Turro, C. New  
34 Ru(II) Complex for Dual Photochemotherapy: Release of Cathepsin K Inhibitor and  $^1\text{O}_2$   
35 Production. *Dalton Trans.* **2018**, *47*, 11851–11858.  
36  
37 58. Phillips, T.; Haq, I.; Meijer, A. J. H. M.; Adams, H.; Soutar, I.; Swanson, L.; Sykes, M. J.;  
38 Thomas, J. A. DNA Binding of an Organic dppz-Based Intercalator. *Biochemistry* **2004**,  
39 *43*, 13657–13665.  
40  
41 59. Bellin, D. L.; Sakhtah, H.; Rosenstein, J. K.; Levine, P. M.; Thimot, J.; Emmett, K.;  
42 Dietrich, L. E. P.; Shepard, K. L. Integrated Circuit-Based Electrochemical Sensor for  
43 Spatially Resolved Detection of Redox-Active Metabolites in Biofilms. *Nat. Commun.*  
44 **2014**, *5*, 3256.  
45  
46 60. Humeniuk, H. V.; Rosspeintner, A.; Licari, G.; Kilin, V.; Bonacina, L.; Vauthey, E.; Sakai,  
47 N.; Matile, S. White-Fluorescent Dual-Emission Mechanosensitive Membrane Probes that  
48 Function by Bending Rather than Twisting. *Angew. Chem. Int. Ed.* **2018**, *57*, 10559–10563.  
49  
50 61. Schindler, J.; Traber, P.; Zedler, L.; Zhang, Y.; Lefebvre, J.-F.; Kupfer, S.; Gräfe, S.;  
51 Demeunynck, M.; Chavarot-Kerlidou, M.; Dietzek, B. Photophysics of a Ruthenium  
52 Complex with a  $\pi$ -Extended Dipyridophenazine Ligand for DNA Quadruplex Labeling. *J.*  
53 *Phys. Chem. A* **2018**, *122*, 6558–6569.  
54  
55  
56  
57  
58  
59  
60

- 1  
2  
3 62. Okamoto, T.; Terada, E.; Kozaki, M.; Uchida, M.; Kikukawa, S.; Okada, K. Facile  
4 Synthesis of 5,10-Diaryl-5,10-dihydrophenazines and Application to EL Devices. *Org.*  
5 *Lett.* **2003**, *5*, 373–376.  
6  
7 63. Liu, Q.; Zhao, C.; Tian, G.; Ge, H. Changing Molecular Conjugation with a Phenazine  
8 Acceptor for Improvement of Small Molecule-Based Organic Electronic Memory  
9 Performance. *RSC Adv.* **2018**, *8*, 805–811.  
10  
11 64. Day, N. U.; Walter, M. G.; Wamser, C. C. Preparations and Electrochemical  
12 Characterizations of Conductive Porphyrin Polymers. *J. Phys. Chem. C* **2015**, *119*, 17378–  
13 17388.  
14  
15 65. Koyama, D.; Dale, H. J. A.; Orr-Ewing, A. J. Ultrafast Observation of a Photoredox  
16 Reaction Mechanism: Photoinitiation in Organocatalyzed Atom-Transfer Radical  
17 Polymerization. *J. Am. Chem. Soc.* **2018**, *140*, 1285–1293.  
18  
19 66. Shi, J.; Chen, J.; Chai, Z.; Wang, H.; Tang, R.; Fan, K.; Wu, M.; Han, H.; Qin, J.; Peng,  
20 T.; Li, Q.; Li, Z. High Performance Organic Sensitizers Based on 11,12-  
21 Bis(hexyloxy)dibenzo[*a,c*]phenazine for Dye-Sensitized Solar Cells. *J. Mater. Chem.*  
22 **2012**, *22*, 18830–18838.  
23  
24 67. Richard, C. A.; Pan, Z.; Hsu, H.-Y.; Cekli, S.; Schanze, K. S.; Reynolds, J. R. Effect of  
25 Isomerism and Chain Length on Electronic Structure, Photophysics, and Sensitizer  
26 Efficiency in Quadrupolar (Donor)<sub>2</sub>-Acceptor Systems for Application in Dye-Sensitized  
27 Solar Cells. *ACS Appl. Mater. Interfaces* **2014**, *6*, 5221–5227.  
28  
29 68. Huang, Z.-S.; Zang, X.-F.; Hua, T.; Wang, L.; Meier, H.; Cao, D. 2,3-Dipentylidithieno[3,2-  
30 *f*:2',3'-*h*]quinoxaline-Based Organic Dyes for Efficient Dye-Sensitized Solar Cells: Effect  
31 of  $\pi$ -Bridges and Electron Donors on Solar Cell Performance. *ACS Appl. Mater. Interfaces*  
32 **2015**, *7*, 20418–20429.  
33  
34 69. Murali, M. G.; Wang, X.; Wang, Q.; Valiyaveetil, S. Design and Synthesis of New  
35 Ruthenium Complex for Dye-Sensitized Solar Cells. *RSC Adv.* **2016**, *6*, 57872–57879.  
36  
37 70. Huang, L.; Ma, P.; Deng, G.; Zhang, K.; Ou, T.; Lin, Y.; Wong, M. S. Novel Electron-  
38 Deficient Quinoxalinedithienothiophene- and Phenazinedithienothiophene-Based  
39 Photosensitizers: The Effect of Conjugation Expansion on DSSC Performance. *Dyes Pigm.*  
40 **2018**, *159*, 107–114.  
41  
42 71. Anderson, H. L. *meso*-Alkynyl Porphyrins. *Tetrahedron Lett.* **1992**, *33*, 1101–1104.  
43  
44 72. Arnold, D. P.; Nitschinsk, L. J. Porphyrin Dimers Linked by Conjugated Butadiynes.  
45 *Tetrahedron* **1992**, *48*, 8781–8792.  
46  
47 73. Arnold, D. P.; Manno, D.; Micocci, G.; Serra, A.; Tepore, A.; Valli, L. Porphyrin Dimers  
48 Linked by a Conjugated Alkyne Bridge: Novel Moieties for the Growth of Langmuir–  
49 Blodgett Films and Their Applications in Gas Sensors. *Langmuir* **1997**, *13*, 5951–5956.  
50  
51 74. Arnold, D. P.; James, D. A. Dimers and Model Monomers of Nickel(II)  
52 Octaethylporphyrin Substituted by Conjugated Groups Comprising Combinations of Triple  
53 Bonds with Double Bonds and Arenes. 1. Synthesis and Electronic Spectra. *J. Org. Chem.*  
54 **1997**, *62*, 3460–3469.  
55  
56  
57  
58  
59

- 1  
2  
3 75. Maretina, I. A. Porphyrin–Ethyne Arrays: Synthesis, Design, and Application. *Russ. J. Gen. Chem.* **2009**, *79*, 1544–1581.
- 4  
5  
6 76. Shinokubo, H.; Osuka, A. Marriage of Porphyrin Chemistry with Metal-Catalysed Reactions. *Chem. Commun.* **2009**, 1011–1021.
- 7  
8  
9 77. Susumu, K.; Therien, M. J. Design of Diethynyl Porphyrin Derivatives with High Near Infrared Fluorescence Quantum Yields. *J. Porphyrins Phthalocyanines* **2015**, *19*, 205–218.
- 10  
11 78. Rickhaus, M.; Jentzsch, A. V.; Tejerina, L.; Grübner, I.; Jirasek, M.; Claridge, T. D. W.; Anderson, H. L. Single-Acetylene Linked Porphyrin Nanorings. *J. Am. Chem. Soc.* **2017**, *139*, 16502–16505.
- 12  
13  
14  
15 79. Lu, X.; Fan, S.; Wu, J.; Jia, X.; Wang, Z.-S.; Zhou, G. Controlling the Charge Transfer in D–A–D Chromophores Based on Pyrazine Derivatives. *J. Org. Chem.* **2014**, *79*, 6480–6489.
- 16  
17  
18  
19 80. Higashino, T.; Imahori, H. Porphyrins as Excellent Dyes for Dye-Sensitized Solar Cells: Recent Developments and Insights. *Dalton Trans.* **2015**, *44*, 448–463.
- 20  
21 81. Zhang, C.-R.; Li, X.-Y.; Shen, Y.-L.; Wu, Y.-Z.; Liu, Z.-J.; Chen, H.-S. Molecular Docking toward Panchromatic Dye Sensitizers for Solar Cells Based upon Tetraazulenylporphyrin and Tetraanthracenylporphyrin. *J. Phys. Chem. A* **2017**, *121*, 2655–2664.
- 22  
23  
24  
25 82. Takanami, T.; Wakita, A.; Sawaizumi, A.; Iso, K.; Onodera, H.; Suda, K., One-Pot Synthesis of *meso*-Formylporphyrins by S<sub>N</sub>Ar Reaction of 5,15-Disubstituted Porphyrins with (2-Pyridyldimethylsilyl)methylolithium. *Org. Lett.* **2008**, *10*, 685–687.
- 26  
27  
28  
29 83. Yu, L.; Muthukumar, K.; Sazanovich, I. V.; Kirmaier, C.; Hindin, E.; Diers, J. R.; Boyle, P. D.; Bocian, D. F.; Holten, D.; Lindsey, J. S. Excited-State Energy-Transfer Dynamics in Self-Assembled Triads Composed of Two Porphyrins and an Intervening Bis(dipyrrinato)metal Complex. *Inorg. Chem.* **2003**, *42*, 6629–6647.
- 30  
31  
32  
33 84. Lindsey, J. S.; Wagner, R. W. Investigation of the Synthesis of Ortho-Substituted Tetraphenylporphyrins. *J. Org. Chem.* **1989**, *54*, 828–836.
- 34  
35  
36  
37 85. Sheridan, M. V.; Lam, K.; Geiger, W. E. Covalent Attachment of Porphyrins and Ferrocenes to Electrode Surfaces through Direct Anodic Oxidation of Terminal Ethynyl Groups. *Angew. Chem. Int. Ed.* **2013**, *52*, 12897–12900.
- 38  
39  
40  
41 86. High, J. S.; Virgil, K. A.; Jakubikova, E. Electronic Structure and Absorption Properties of Strongly Coupled Porphyrin–Perylene Arrays. *J. Phys. Chem. A* **2015**, *119*, 9879–9888.
- 42  
43  
44 87. Koenigsmann, C.; Ripolles, T. S.; Brennan, B. J.; Negre, C. F. A.; Koepf, M.; Durrell, A. C.; Milot, R. L.; Torre, J. A.; Crabtree, R. H.; Batista, V. S.; Brudvig, G. W.; Bisquert, J.; Schmittenmaer, C. A. Substitution of a Hydroxamic Acid Anchor into the MK-2 Dye for Enhanced Photovoltaic Performance and Water Stability in a DSSC. *Phys. Chem. Chem. Phys.* **2014**, *16*, 16629–16641.
- 45  
46  
47  
48  
49  
50 88. Sawyer, D. T.; Sobkowiak, A.; Roberts, J. L., Jr. *Electrochemistry for Chemists*. 2nd ed.; John Wiley & Sons, Inc.: New York, **1995**.
- 51  
52  
53 89. Becke, A. D. Density-Functional Thermochemistry. III. The Role of Exact Exchange. *J. Phys. Chem.* **1993**, *98*, 5648–5652.
- 54  
55  
56  
57  
58  
59  
60

- 1  
2  
3 90. Weigend, F.; Ahlrichs, R. Balanced Basis Sets of Split Valence, Triple Zeta Valence and  
4 Quadruple Zeta Valence Quality for H to Rn: Design and Assessment of Accuracy. *Phys.*  
5 *Chem. Chem. Phys.* **2005**, *7*, 3297–3305.  
6  
7 91. Frisch, M. J.; Trucks, G. W.; Schlegel, H. B.; Scuseria, G. E.; Robb, M. A.; Cheeseman, J.  
8 R.; Scalmani, G.; Barone, V.; Mennucci, B.; Petersson, G. A.; Nakatsuji, H.; Caricato, M.;  
9 Li, X.; Hratchian, H. P.; Izmaylov, A. F.; Bloino, J.; Zheng, G.; Sonnenberg, J. L.; Hada,  
10 M.; Ehara, M.; Toyota, K.; Fukuda, R.; Hasegawa, J.; Ishida, M.; Nakajima, T.; Honda, Y.;  
11 Kitao, O.; Nakai, H.; Vreven, T.; Montgomery, J. A., Jr.; ; Peralta, J. E.; Ogliaro, F.;  
12 Bearpark, M.; Heyd, J. J.; Brothers, E.; Kudin, K. N.; Staroverov, V. N.; Kobayashi, R.;  
13 Normand, J.; Raghavachari, K.; Rendell, A.; Burant, J. C.; Iyengar, S. S.; Tomasi, J.; Cossi,  
14 M.; Rega, N.; Millam, J. M.; Klene, M.; Knox, J. E.; Cross, J. B.; Bakken, V.; Adamo, C.;  
15 Jaramillo, J.; Gomperts, R.; Stratmann, R. E.; Yazyev, O.; Austin, A. J.; Cammi, R.;  
16 Pomelli, C.; Ochterski, J. W.; Martin, R. L.; Morokuma, K.; Zakrzewski, V. G.; Voth, G.  
17 A.; Salvador, P.; Dannenberg, J. J.; Dapprich, S.; Daniels, A. D.; Farkas, Ö.; Foresman, J.  
18 B.; Ortiz, J. V.; Cioslowski, J.; Fox, D. J. *Gaussian 09*, Gaussian, Inc.: Wallingford CT,  
19 **2009**.  
20  
21 92. Furche, F.; Ahlrichs, R. Adiabatic Time-Dependent Density Functional Methods for  
22 Excited State Properties. *J. Chem. Phys.* **2002**, *117*, 7433–7447.  
23  
24 93. Marenich, A. V.; Cramer, C. J.; Truhlar, D. G. Universal Solvation Model Based on Solute  
25 Electron Density and on a Continuum Model of the Solvent Defined by the Bulk Dielectric  
26 Constant and Atomic Surface Tensions. *J. Phys. Chem. B* **2009**, *113*, 6378–6396.  
27  
28 94. Martin, R. L. Natural Transition Orbitals. *J. Chem. Phys.* **2003**, *118*, 4775–4777.  
29  
30  
31  
32  
33  
34  
35  
36  
37  
38  
39  
40  
41  
42  
43  
44  
45  
46  
47  
48  
49  
50  
51  
52  
53  
54  
55  
56  
57  
58  
59  
60